RECOVERING OBSERVABILITY VIA ACTIVE SENSING

by

Abhinav Srinivas Sai Kiran Kunapareddy

A thesis submitted to The Johns Hopkins University in conformity with the requirements for the degree of Master of Science.

Baltimore, Maryland

May, 2016

Abstract

Observability is a formal property of a system that ensures the ability to estimate the system's states from output measurements and knowledge of the inputs. Even when state estimators are not employed, observability is a crucial property in the design of feedback control systems. Engineering sensors are typically designed to guarantee observability irrespective of the control input, thereby simplifying control systems design. Here, we introduce a class of nonlinear sensors that require 'persistently exciting' control inputs to maintain observability. This class of sensor models is motivated by biological sensing systems which 'adapt' to constant stimuli, giving them a very high dynamic range, but leading to a phenomenon known as perceptual fading.

To prevent perceptual fading, animals employ *active sensing behaviors* in the form of time-varying motor commands that continually stimulate sensory receptors. To capture this phenomenon, we introduce a simplified sensor model that requires similar 'active' control inputs to maintain observability. Under certain assumptions, the input–output characteristics of the active sensing system is shown to be equiva-

ABSTRACT

lent to an observable LTI system. Specifically, we apply three steps to the original (nonlinear) system—(1) modulating via sinusoidal active input, (2) demodulating, and (3) low-pass filtering. The equivalent system is identified by analyzing the Harmonic Transfer Function (HTF) of the modulated system and whose output is then demodulated and low pass filtered. Equivalence of the new observable LTI system and the active sensing system illustrates the potential effectiveness of this framework for active sensing and may pave the way for the design of adaptive sensory systems for engineering applications.

Primary Reader: Noah J. Cowan

Secondary Readers: M. Mert Ankarali, Eric S. Fortune

Acknowledgments

The first person I express my thanks to has to be Dr. Noah Cowan, for being the amazing advisor he has been. His support through the entire year kept me motivated and focused.

Apart from my advisor, I would also like to thank Dr. Eric Fortune and Dr. M. Mert Ankarali for their valuable comments and feedback on the thesis.

Contents

Abstract **ii**

Acknowledgments **iv**

List of Tables **vii**

List of Figures **viii**

1 Introduction **1**

1.1 Scope of Research 2

2 Active Sensing **4**

2.1 Active Sensing in Biology 4

2.2 The "Simplest" System Requiring Active Sensing 5

2.3 Why Active Sensing? 6

2.4 Our System with Active Sensing 9

3 Harmonic Transfer Functions for the "Simplest" Active Sensing Sys-

tem **11**

3.1 State Space Representation of HTF 13

3.2 HTF's for Our Active Sensing System 14

4 Proposed Framework **17**

4.1 Extracting the Observable Harmonic 18

4.2 Resulting Equivalent System 19

4.3 Simulation 19

4.3.1 System and Filter Parameters 20

4.3.2 State Estimation and Control 21

4.4 Results 22

4.4.1 System Identification of Nonlinear System 22

4.4.2 LQG Control 22

4.4.3 Approximation Degrades at High Frequency 23

5 Summary **27**

A Always Unobservable Sensory Scene **29**

B HTF of the System Using Impulse Response Functions **31**

Bibliography **34**

Vita **43**

List of Tables

4.1 System and sensory scene parameters. 20
4.2 Kalman filter parameters. 21
4.3 LQR parameters. 21

List of Figures

3.1 The input-output relation of an LTP system visualized via infinitely many LTI harmonics. 12

4.1 Comparing the actual system to approximately equivalent system. . 20
4.2 Comparison of the Bode-plots of the nonlinear system and the approximately equivalent linear system developed using parameters in Table 4.1. 23
4.3 Simulation and comparison of system states and outputs to validate the developed framework. Note that for this regime, the linear simulation (panels a-c) closely matches the nonlinear system. 24
4.4 Comparison of the output signals for various sinusoidal frequencies for the input, δu. Note that when the input frequency approaches and exceeds the pumping frequency of u^* the linear simulation deviates substantially from the nonlinear simulation, as expected. 25

Chapter 1

Introduction

The dominant paradigm in feedback control theory is to decouple the problems of control and state estimation. This is called the separation principle. For example, for a linear plant corrupted with a Gaussian noise a Kalman filter can be used for optimal state estimation, which can then be used to drive a linear-quadratic regulator (LQR). The separation principle allows us to design the Kalman filter and controller independently of one another; i.e., the Kalman filter does not depend on the LQR cost function, and the LQR gains do not depend on the sensory and process noise covariances.

However, for a general nonlinear plant the separation principle does not hold. So, in order to facilitate the design of independent observers and controllers it may—or may not—be a good idea to start with linearization. For example, for a simple nonlinearity (say a sinusoid close to the origin) in the states of the system, it may

be a good idea to linearize the system around its equilibrium. However, certain categories of nonlinearities may preclude linear separability even if the system is both (nonlinearly) controllable and observable.

Indeed, we suspect that this paradigm (linearization as the first step in control design) does not apply to many biological control systems in animals. Biological sensory systems often stop responding to persistent (i.e. "DC") stimuli, a process known as "adaptation" in the neuroscience literature. Sensory adaptation makes asymptotically exact set-point control impossible due to the imperceptibility of large, slow drifts in the signal of interest. Animals often use a strategy known as active sensing [1–3] in which the organism generates potentially costly movements that do not necessarily directly serve a motor goal but improve sensory feedback and prevent perceptual fading [4]. Indeed, any searching behavior is a form of active sensing and many species of animals perform such behaviors. This thesis focuses on developing a framework to use such active sensing movements to recover the observability for a simple biologically inspired nonlinear system.

1.1 Scope of Research

Our central hypothesis is that the movements of an active sensing system can be used to recover the observability of the system thereby improving task-level control performance. In Chapter 2, we will develop and describe a simple biologically inspired

system which requires active sensing. Once the need for active sensing is established, we derive a new LTP system by linearizing the system around the "active" movements. In Chapter 3, we then simplify the LTP system using Harmonic Transfer Function (HTF) theory. In Chapter 4, we develop a framework to derive an approximately equivalent LTI system (via demodulation and low-pass filtering). To demonstrate the potential effectiveness of this approach, we control a simulated nonlinear system via active sensing in conjunction with a control law designed for the LTI approximation. Chapter 5, concludes with a summary and suggestions for possible future work than can extend and improve upon this framework.

Chapter 2

Active Sensing

2.1 Active Sensing in Biology

Active sensing can be broadly defined as a feedback controlled system that expends energy to sense its surroundings [1, 2]. Active sensing is most commonly associated with species that generate and emit sensing signals, such as echolocation in bats [5,6] or active electroreception in certain species of fish [7]. However, a more general form of active sensing involves energy expenditure via the system's own active movements [8–17]. Some examples of movement-based active sensing are movements of weakly electric fish [3, 18–21], active sensing in vision [22–24], whisking [25–29], active touch [30–33], sniffing [34–36] and hydrodynamic imaging [37–39].

During the course of such movement-based active sensing, the animal's motor behavior does not linearly relate to its task-level goal and is often routinely changed in

relation to the sensory demands [40–46]. This suggests that animal's movement might be stimulating/altering the sensory signals it is receiving in order to better excite its sensors and downstream neural circuits, thereby improve task-level performance [3].

The fundamental goal of our work is to examine, using simplified models and mathematical analysis, how active movements of a system, even if not directly related to the task, can nevertheless be used to improve the task-level performance in achieving a motor goal.

2.2 The "Simplest" System Requiring Active Sensing

In this section we introduce a simple (perhaps the simplest) biologically inspired sensory system that, when coupled with a mechanical system, requires active sensing to ensure observability. This model is motivated by ongoing studies of sensorimotor control in weakly electric knifefish in the LIMBS Laboratory in a simple one-degree-of-freedom refuge tracking behavior [3, 47–50].

Suppose x_1 is the position of the system and $x_2 = \dot{x}_1$ is its velocity as it moves in one degree of freedom according to the simple dynamics $m\dot{x}_2 + bx_2 = u$ as described for weakly electric fish [48]. To formalize the notion of sensory adaptation, we assume a receptor measures only the local rate of change of a stimulus as the system moves relative to a sensory scene $s(x_1)$, i.e., $y = \frac{d}{dt}s(x_1)$. Defining $g(x_1) = s'(x_1)$, we arrive

at the following model:

$$\begin{aligned} \dot{x} &= \underbrace{\begin{bmatrix} 0 & 1 \\ 0 & -\frac{b}{m} \end{bmatrix}}_{\text{A}} x + \underbrace{\begin{bmatrix} 0 \\ \frac{1}{m} \end{bmatrix}}_{\text{B}} u, \\ y &= g(x_1)x_2, \end{aligned} \tag{2.1}$$

where m is the mass and b is the damping.

2.3 Why Active Sensing?

The linearization of (2.1) around any equilibrium, $(x_1^*, 0)$, is given by (A, B, C), where

$$\begin{aligned} A &= \begin{bmatrix} 0 & 1 \\ 0 & -\frac{b}{m} \end{bmatrix}, \quad B = \begin{bmatrix} 0 \\ \frac{1}{m} \end{bmatrix}, \\ C &= \begin{bmatrix} 0 & g(x_1^*) \end{bmatrix}. \end{aligned} \tag{2.2}$$

Clearly, (A, C) is not observable irrespective of $g(x)$. The observability matrix of the system always looses rank due to output being proportional to the velocity of the sensor, making it impossible to infer its position (since the system is translationally invariant).[1]

[1]Note that if the system had a "spring-like term" in the (2,1) entry of the A matrix, observability would be recovered [51].

However, a simple rank condition test [52] on the nonlinear system, as illustrated below shows that nonlinear observability is guaranteed for nonzero velocities, $x_2 \neq 0$:

$$\dot{x} = Ax + Bu,$$

$$y = g(x_1)x_2.$$

The Lie derivatives of the system are given by

$$\begin{aligned}
h &= g(x_1)x_2, \\
L_f h &= \frac{\partial h}{\partial x} f \\
&= \begin{bmatrix} g'(x_1)x_2 & g(x_1) \end{bmatrix} Ax \\
&= \begin{bmatrix} g'(x_1)x_2 & g(x_1) \end{bmatrix} \begin{bmatrix} 0 & 1 \\ 0 & \frac{-b}{m} \end{bmatrix} \begin{bmatrix} x_1 \\ x_2 \end{bmatrix} \\
&= \begin{bmatrix} 0 & g'(x_1)x_2 - g(x_1)\frac{b}{m} \end{bmatrix} \begin{bmatrix} x_1 \\ x_2 \end{bmatrix} \\
&= g'(x_1)x_2^2 - g(x_1)x_2\frac{b}{m}.
\end{aligned}$$

Following [52], we define the matrix G via

$$\begin{aligned} G &= \begin{bmatrix} h \\ L_f h \end{bmatrix} \\ &= \begin{bmatrix} g(x_1)x_2 \\ g'(x_1)x_2^2 - g(x_1)x_2\frac{b}{m} \end{bmatrix} \\ &= \begin{bmatrix} g'(x_1)x_2 & g(x_1) \\ g'(x_1)x_2^2 - g(x_1)x_2\frac{b}{m} & 2g'(x_1)x_2 - g(x_1)\frac{b}{m} \end{bmatrix}. \end{aligned}$$

For the system to be nonlinearly observable we require that G be full rank, which is guaranteed for nonzero determinant:

$$x_2^2(2(g'(x_1))^2 - g(x_1)g''(x_1)) \neq 0. \tag{2.3}$$

This simple result illustrates that control to a fixed position ($x_2 = 0$) results in a loss of not just linear observability, but also of *nonlinear observability*—i.e. it is a fundamental system property and not an artifact of linearization. And thus, to maintain observability, one must design a control input that sufficiently excites the sensory system to enable estimation of the states necessary for control. Similar ideas have been explored in previous work [53, 54].

2.4 Our System with Active Sensing

In this section, we try to excite the sensory system ("pumping" the system) with a time-periodic control signal $u^*(t)$. This is equivalent to linearizing the system (2.1) around a time varying equilibrium $(x^*(t), u^*(t))$ which results in the following approximate LTV system around the equilibrium $(x^*(t), u^*(t))$:

$$\begin{aligned}
\dot{\delta x} &= A\delta x + B\delta u, \\
\delta y &= \left[\begin{array}{cc} \frac{\partial}{\partial x_1} g(x_1)x_2 & \frac{\partial}{\partial x_2} g(x_1)x_2 \end{array}\right]_{x=x^*} \delta x, \\
&= \left[\begin{array}{cc} g'(x_1^*)x_2^* & g(x_1^*) \end{array}\right] \delta x.
\end{aligned}$$

Choosing $x_1^* = \cos(\omega t)$ results in the equilibrium state $(x^*(t), u^*(t))$ given by

$$\begin{aligned}
x^*(t) &= \left[\begin{array}{c} x_1^*(t) \\ \\ \frac{d}{dt}x_1^*(t) \end{array}\right] = \left[\begin{array}{c} \cos(\omega t) \\ \\ -\omega \sin(\omega t) \end{array}\right], \\
u^*(t) &= -m\omega^2 \cos(\omega t) - b\omega \sin(\omega t),
\end{aligned}$$

where m, b are the mass and damping of the system as specified in (2.1) Thus the resulting LTP system is

$$\begin{aligned}
\dot{\delta x} &= A\delta x + B\delta u, \\
\delta y &= C(t)\delta x,
\end{aligned} \tag{2.4}$$

where A, B are given by (2.2) and

$$C(t) = \begin{bmatrix} g'\left(\cos(\omega t)\right)\omega\sin(\omega t) & g\left(\cos(\omega t)\right) \end{bmatrix}.$$

To simplify notation, we will henceforth be representing δu as u and the total input to the system as $u_{\text{total}} = u + u^*$. Therefore the LTP system now is,

$$\begin{aligned} \dot{\delta x} &= A\delta x + Bu, \\ \delta y &= C(t)\delta x. \end{aligned} \tag{2.5}$$

This LTP system is now further analyzed and simplified using Harmonic Transfer Function (HTF) theory summarized in Chapter 3.

Chapter 3

Harmonic Transfer Functions for the "Simplest" Active Sensing System

Transfer functions are an important tool in the analysis of Linear Time Invariant (LTI) systems. An analogous tool for the analysis of LTP systems are Harmonic Transfer Functions (HTFs) [55–58].

The analysis of LTI systems is often simplified by the simple fact that a sinusoidal input results in a sinusoidal output of the same frequency. However, the frequency response of an LTP system not only includes the input frequency, but also the input frequency plus multiples of the fundamental frequency of the LTP system. By using exponentially modulated periodic form of the input and output signals and

the principle of harmonic balance, Wereley and Hall [55] showed that input–output relationship of a LTP system are determined by a possibly infinite parallel series of frequency shifted LTI sub-systems. The transfer functions of these LTI sub-systems are called the HTFs of the LTP system. Figure 3.1 illustrates the resulting HTF structure (original source Möllerstedt [59]).

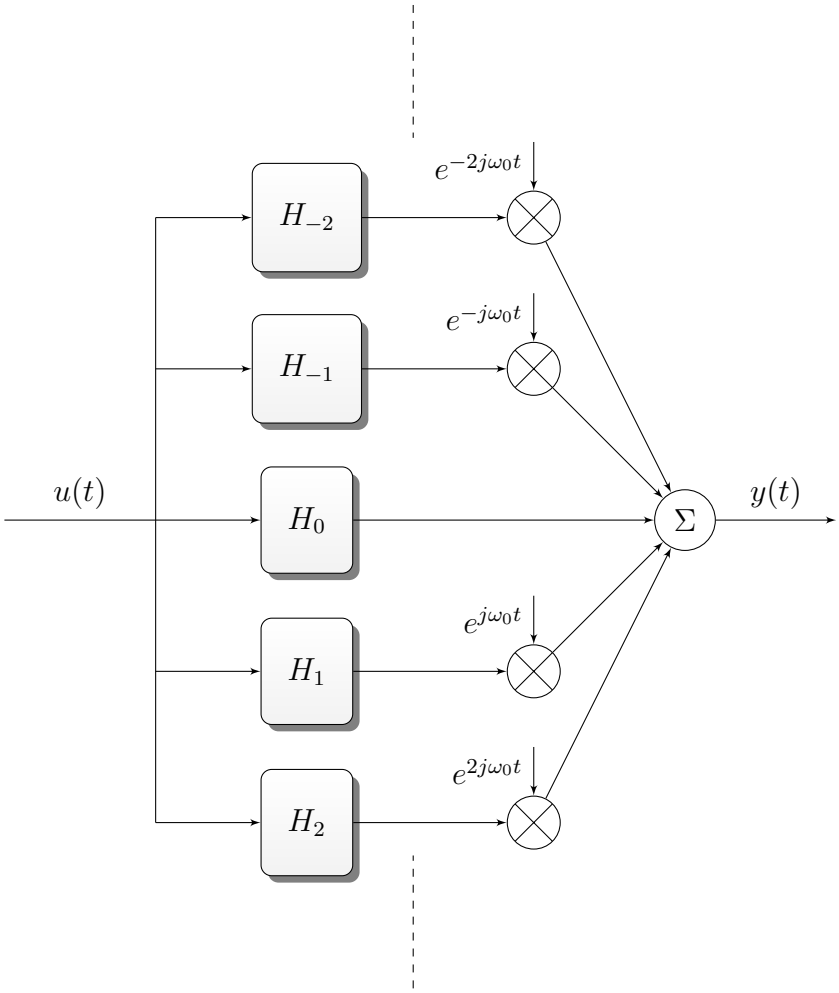

Figure 3.1: The input-output relation of an LTP system visualized via infinitely many LTI harmonics.

3.1 State Space Representation of HTF

A generic LTP system can be defined as,

$$\begin{aligned} \dot{x}(t) &= A(t)x(t) + B(t)u(t), \\ y(t) &= C(t)x(t) + D(t)u(t). \end{aligned} \tag{3.1}$$

For such a system, Wereley and Hall [55] derived the Harmonic transfer functions using the state space representation and the principle of Harmonic Balance, which we review here. This representation is given by

$$\mathcal{H}(s) = \mathcal{C}\left[sI - (\mathcal{A} - \mathcal{N})^{-1}\right]\mathcal{B} + \mathcal{D}, \tag{3.2}$$

where $\mathcal{A}$ is the doubly infinite Toeplitz matrix containing the Fourier coefficients of the the system matrices $A(t)$:

$$\mathcal{A} = \begin{bmatrix} \dots & \vdots & \vdots & \vdots & \dots \\ \dots & A_0 & A_{-1} & A_{-2} & \dots \\ \dots & A_1 & A_0 & A_{-1} & \dots \\ \dots & A_2 & A_1 & A_0 & \dots \\ \dots & \vdots & \vdots & \vdots & \dots \end{bmatrix}. \tag{3.3}$$

and $\mathcal{H}(s)$ is given by

$$\mathcal{H}(s) = \begin{bmatrix} \dots & \vdots & \vdots & \vdots & \dots \\ \dots & H_{-1,-1}(s) & H_{-1,0}(s) & H_{-1,1}(s) & \dots \\ \dots & H_{0,-1}(s) & H_{0,0}(s) & H_{0,1}(s) & \dots \\ \dots & H_{1,-1}(s) & H_{1,0}(s) & H_{1,1}(s) & \dots \\ \dots & \vdots & \vdots & \vdots & \dots \end{bmatrix}. \tag{3.4}$$

Wereley and Hall [55] also showed that the elements $H_{n,m}(s)$ and the transfer functions of the LTI subsystems are related via $H_{n,m}(s) = H_{n-m}(s + jm\omega)$.

The matrices $\mathcal{B}$, $\mathcal{C}$,$\mathcal{D}$ are also represented using doubly infinite Toeplitz matrices containing the Fourier coefficients of the system matrices $B(t)$, $C(t)$, $D(t)$ respectively.

3.2 HTF's for Our Active Sensing System

Equation (3.2), for the simplifying case of time-constant A, B and time-varying C, reduces to the case of "LTI plant with modulated output" as described in [55], and has the following form:

$$\mathcal{H}_{n,m}(s) = C_{n-m} \left(s_m I - A\right)^{-1} B, \tag{3.5}$$

where $\mathcal{H}_{n,m}(s)$ are the elements of the doubly infinite $\mathcal{H}(s)$ and C_k's are the Fourier coefficients of $C(t)$.

To find the analytical expressions for the harmonics, we assume the following form for the sensory scene being observed by the system:

$$\begin{aligned} s(x_1) &= \frac{1}{2} d_1 x_1^2 + e_1 x_1, \\ \implies g(x_1) &= s'(x_1) = d_1 x_1 + e_1, \end{aligned} \tag{3.6}$$

where, d_1 and e_1 are arbitrary real coefficients.

Now for the system (2.5), the Fourier coefficients of C_k's of $C(t)$ are given by,

$$C_0 = \begin{bmatrix} 0 & e_1 \end{bmatrix}, \qquad C_1 = \begin{bmatrix} -\omega\frac{jd_1}{2} & \frac{d_1}{2} \end{bmatrix}, \qquad C_{-1} = \begin{bmatrix} \omega\frac{jd_1}{2} & \frac{d_1}{2} \end{bmatrix}. \tag{3.7}$$

This gives the following form for the HTFs from (3.5):

$$H_0(s) = \frac{e_1}{b + Ms}, \qquad H_1(s) = \frac{d_1(s + j\omega)}{2s(b + Ms)}, \qquad H_{-1}(s) = \frac{d_1(s - j\omega)}{2s(b + Ms)}. \tag{3.8}$$

The output of the LTP system (2.5) can now be represented as

$$\delta y = h_0 \ast u + (h_1 \ast u)e^{j\omega t} + (h_{-1} \ast u)e^{-j\omega t}, \tag{3.9}$$

where h_0, h_1, h_{-1} are the time-domain representations of $H_0(s)$, $H_1(s)$, $H_{-1}(s)$ respectively and $\ast$ denotes the convolution operation. Note that the sensory scene chosen in this work only contains the zeroth and first harmonics. If the sensory scene were to contain higher harmonics as well, then (3.9) below would only be an approximation

of the original system (2.5) that neglects the higher harmonics. Given our use of low-pass filtering (Chapter 4) this approximation will nevertheless prove useful for more general scenes.

Simplifying (3.9) using $e^{j\omega t} = \cos(\omega t) + j\sin(\omega t)$ and the fact that h_{-1} and h_1 are complex conjugates gives the following:

$$\begin{aligned}\delta y &= h_0 * u + (h_1 * u)e^{j\omega t} + \left[(h_1 * u)e^{j\omega t}\right]^* \\ &= h_0 * u + 2\mathrm{Re}\left[(h_1 * u)e^{j\omega t}\right] \\ &= h_0 * u + 2\left[\mathrm{Re}(h_1 * u)\cos(\omega t) - \mathrm{Im}(h_1 * u)\sin(\omega t)\right].\end{aligned} \tag{3.10}$$

Therefore, using HTF theory the output (2.5) can be simplified to

$$\delta y = h_0 * u + 2\left[\mathrm{Re}(h_1) * u\right]\cos(\omega t) - 2\left[\mathrm{Im}(h_1) * u\right]\sin(\omega t). \tag{3.11}$$

Note that, from Equation (3.8), we have

$$\mathrm{Im}(H_1) = \frac{a}{ms^2 + bs}, \tag{3.12}$$

where $a = (d_1/2)\omega$, has no pole-zero cancellations, a fact used in Chapter 4.

An alternate method to obtain the HTF components for our system using impulse response functions as demonstrated in [59] is shown in Appendix B.

Chapter 4

Proposed Framework

After deriving the HTFs for the active sensing under consideration in Chapter 3, we noted that the imaginary part of first harmonic has no pole-zero cancellations (resulting in an observable system). So, if we were able to successfully extract it, we would be able to use it as the output of a equivalent system which is observable. Indeed, this is the crux of this thesis. This chapter focuses on developing the rest of our framework in order to extract the imaginary part of first harmonic and develop a new LTI system which is approximately equivalent to the original nonlinear system.

4.1 Extracting the Observable Harmonic

As can be seen from the output Equation (3.11),

$$\delta y = h_0 * u + 2\left[\mathrm{Re}(h_1) * u\right]\cos(\omega t) - 2\left[\mathrm{Im}(h_1) * u\right]\sin(\omega t), \tag{4.1}$$

the first harmonic's imaginary part is modulated by a sinusoidal signal. So, we demodulate (3.11) with a sinusoidal signal, which results in the following equation:

$$\begin{aligned}\delta y_{\mathrm{mod}} &= \delta y \sin\omega t \\ &= (h_0 * u)\sin\omega t + (\mathrm{Re}(h_1) * u)\sin 2\omega t + (\cos 2\omega t - 1)\mathrm{Im}(h_1) * u \\ &= -\mathrm{Im}(h_1) * u + (h_0 * u)\sin\omega t + (\mathrm{Re}(h_1) * u)\sin 2\omega t + (\mathrm{Im}(h_1) * u)\cos 2\omega t.\end{aligned} \tag{4.2}$$

After demodulation, we notice that the output is still corrupted by the remaining harmonics (modulated by sinusoids at ω and 2ω). If we assume that $h_0 * u$, $\mathrm{Re}(h_1) * u$, and $\mathrm{Im}(h_1) * u$ are sufficiently band-limited signals, then it is possible, in principle, to low-pass filter δy_{mod}, thereby extracting the first term $\mathrm{Im}(h_1) * u$, which is not modulated. So, we pass the output from (4.2) through a low-pass filter, and assume that the modulated signals are perfectly suppressed, namely

$$\begin{aligned}\delta y_{\mathrm{fil}} &= \delta y_{\mathrm{mod}} * h_{\mathrm{lpf}} \\ &= -h_{\mathrm{lpf}} * \mathrm{Im}(h_1) * u,\end{aligned} \tag{4.3}$$

where h_{lpf} represents the low-pass filter. Note that, apart from filtering the output, the low pass filter must also be included in our model of the dynamics of the system.

4.2 Resulting Equivalent System

The approximate equivalent system is depicted in Figure 4.1b. The transfer function of the "Simplified System" is given by the imaginary part of the first harmonic derived in Chapter 3:

$$\frac{a}{ms^2 + bs}, \tag{3.12}$$

where $a = d_1\omega/2$. This new transfer function has no pole zero cancellations, reflecting the fact that active sensing rendered the system observable.

4.3 Simulation

In order to compare the developed LTI system and the original active sensing system, we simulate both the systems whilst using an LQG controller to control the system to a fixed position. MATLAB has been used to simulate both the system and the controller. The details of the system and sensor parameters, low-pass filter, and the LQG controller used in the simulation are summarized below.

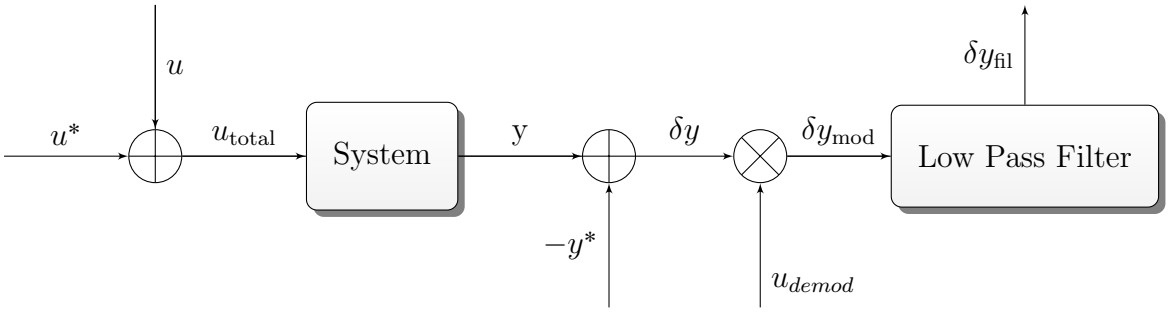

(a) Actual nonlinear system.

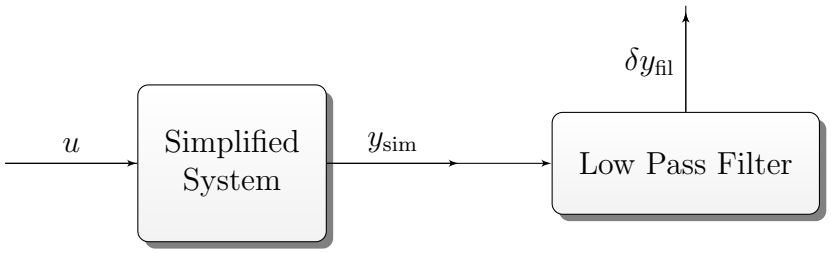

(b) Approximately equivalent system.

Figure 4.1: Comparing the actual system to approximately equivalent system.

4.3.1 System and Filter Parameters

The sensory scene is given by $s(x) = \frac{1}{2}d_1x^2 + e_1x$, introducing two parameters. Furthermore, the LTP plant model (2.5) in Chapter 2 has three parameters (m, b, and ω). The parameters used in our simulations are given in Table 4.1.

Parameter	Description	Value	Units
m	System mass	1	kg
b	System damping	1.7	$\mathrm{N \cdot s \cdot m^{-1}}$
ω	Pumping frequency	$2\pi*2$	$\mathrm{rad \cdot s^{-1}}$
d_1	scene coefficient	3	$\mathrm{m^{-2}}$
e_1	scene coefficient	5	$\mathrm{m^{-1}}$

Table 4.1: System and sensory scene parameters.

The system ratio $\frac{b}{m}$ has been chosen based on the ratios of a weakly electric fish system [48], which has inspired this work. A 5^{th}-order Butterworth filter [60] with

0.5 Hz as a cut-off frequency has been used as the low-pass filter in (4.3).

4.3.2 State Estimation and Control

The Kalman filter (KF) [61] is one of the most widely used state estimation methods for linear systems mainly due to its ease of implementation, optimality (under certain assumptions), and versatility. As the details of its implementation can be found in standard estimation literature, we omit those details here.

Since our equivalent LTI system is observable (no pole-zero cancellations), we can use it as a sensor reading for the Kalman filter so as to estimate the states. The initial covariance matrices for the Kalman filter are given in Table 4.2.

Covariance	Value
system noise	$10^{-4} I_{2\times 2}$
measurement noise	0

Table 4.2: Kalman filter parameters.

The estimated state is now fed through an infinite-horizon linear quadratic regulator (LQR) controller to try to control the system to a fixed goal position. The state and control weights for the LQR controller used are assumed to be as in Table 4.3.

Weights	Value
State weights	$2I_{2\times 2}$
control weight	1

Table 4.3: LQR parameters.

4.4 Results

4.4.1 System Identification of Nonlinear System

To show that the developed LTI system and the nonlinear active sensing system are approximately equivalent, we compare the Bode plots of both systems in Fig. 4.2. Although these plots match each other at most frequencies, the following caveats should be noted:

- At 1 Hz frequency (which is half the "pumping" frequency) there is a mismatch between the Bode plots of the approximate LTI system and the nonlinear system. This may be due to as yet unexplored harmonic interactions between the control signal and the system's own harmonics.
- At higher frequencies, the Bode plots do not match due to interactions of the higher harmonics and the control signal leaking through the low-pass filter.

4.4.2 LQG Control

To further validate our framework, we simulated the LQG system in 4.3. Fig. 4.3a demonstrates that the Kalman state estimate of position, $\widehat{\delta x}_1(t)$, of the approximately equivalent LTI system closely matches the relative position of the nonlinear active sensing system about the "Active" movements of the system, i.e. $\delta x_1(t) = x_1(t) - x_1^*(t)$. The velocity state estimate also matches well (Fig. 4.3b). We also compare

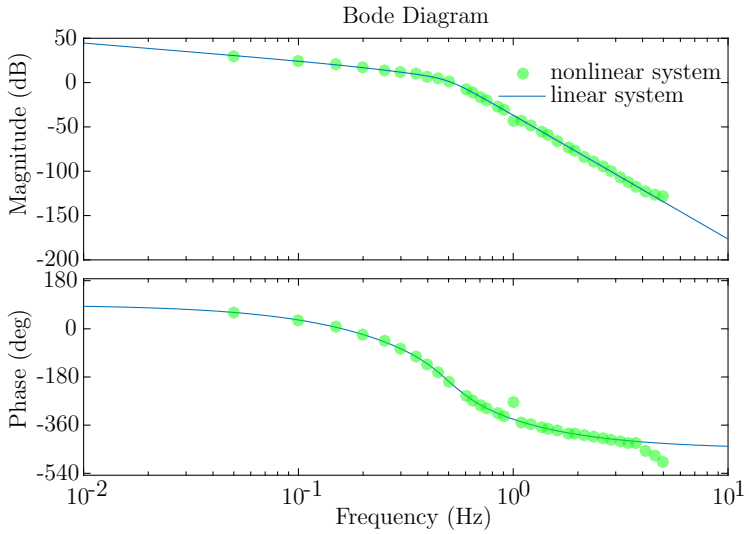

Figure 4.2: Comparison of the Bode-plots of the nonlinear system and the approximately equivalent linear system developed using parameters in Table 4.1.

the output signal from the equivalent LTI system and to the δy_{fil} from the simulation of the nonlinear active sensing system in Fig. 4.3c. Fig. 4.3d plots the position of the system along with it's active movements. This figure also shows how the sensory scene being observed by the system varies with time.

4.4.3 Approximation Degrades at High Frequency

We expect that the LTI approximation should degrade at high frequencies. In Fig. 4.4, to show a few test cases where our developed linear system is no longer approximately equivalent to the nonlinear system, we compare the output signals of both systems, when using a sinusoidal control signal with frequencies close to the system's pumping frequency (these control signals were simulated as a part of the Bode plot generation).

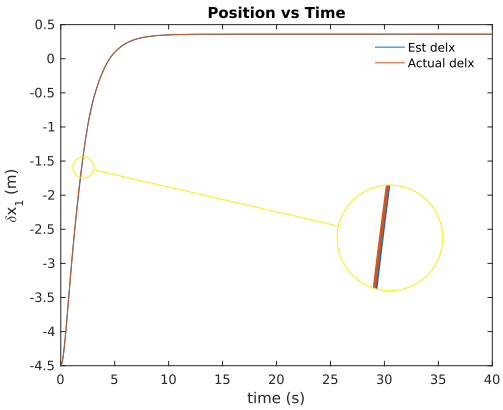

(a) Successful position tracking of the system from an initial position, $\delta x_1 = -4.5$ to $\delta x_1 = 0.36$ using the Kalman position estimate from the approximately equivalent observable system.

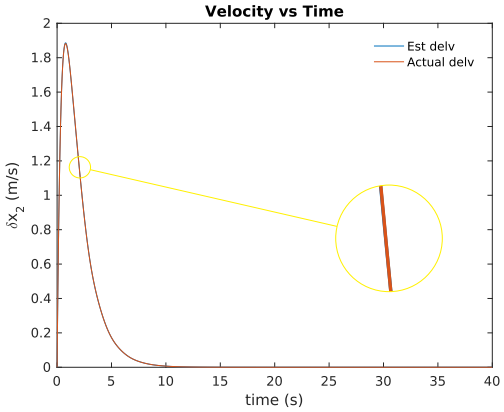

(b) Successful velocity tracking of the system from an initial position, $\delta x_1 = -4.5$ to $\delta x_1 = 0.36$ using the Kalman position estimate from the approximately equivalent observable system.

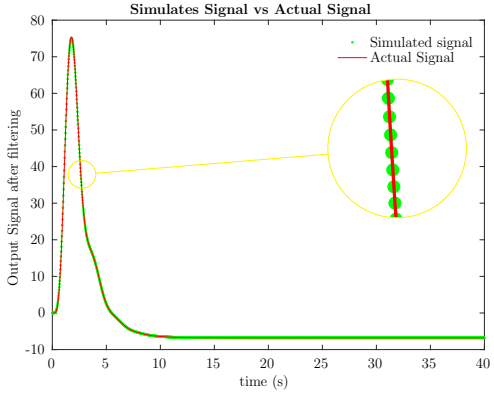

(c) Comparison of the resultant output signal of the nonlinear system to that of the simulated approximate equivalent system when the system is controlled from an initial position, $\delta x_1 = -4.5$ to $\delta x_1 = 0.36$.

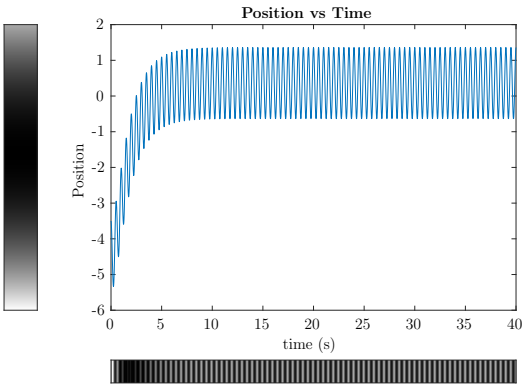

(d) Position of the system w.r.t time when the system is controlled $x_1 = -3.5$ to $x_1 = 1.36$. The color-map attached to x-axis denotes the variation in the intensity of the sensory scene being observed at a particular location and the color-map attached to y-axis denotes the intensity of the sensory scene at an instant.

Figure 4.3: Simulation and comparison of system states and outputs to validate the developed framework. Note that for this regime, the linear simulation (panels a-c) closely matches the nonlinear system.

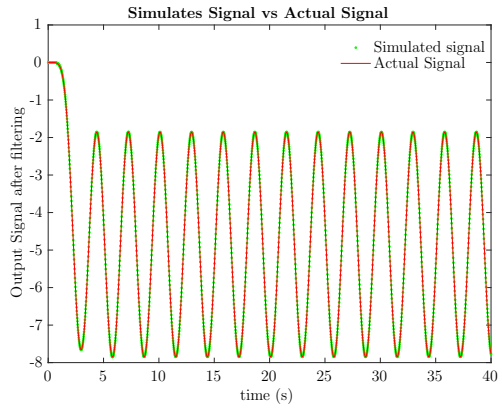

(a) control frequency of 0.35 Hz.

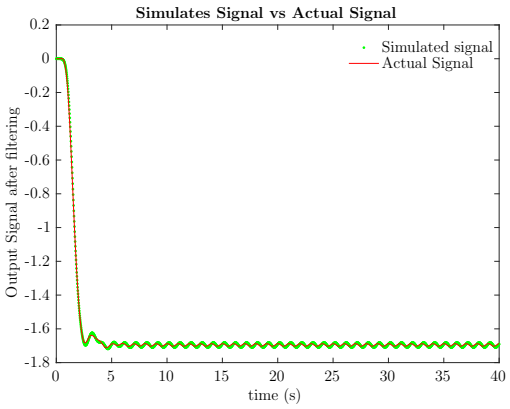

(b) control frequency of 1 Hz.

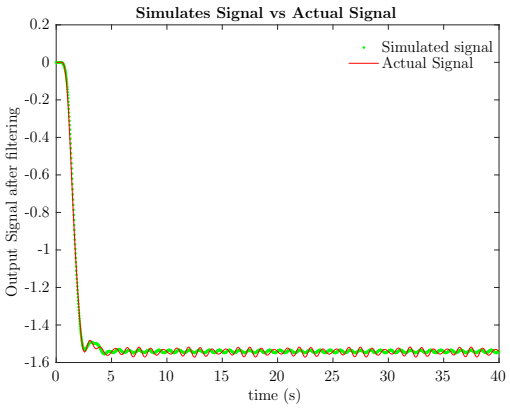

(c) control frequency of 1.1 Hz.

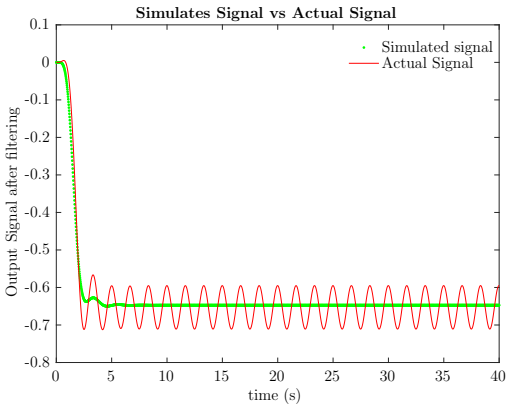

(d) control frequency of 2.6 Hz.

Figure 4.4: Comparison of the output signals for various sinusoidal frequencies for the input, δu. Note that when the input frequency approaches and exceeds the pumping frequency of u^* the linear simulation deviates substantially from the nonlinear simulation, as expected.

The plots in Fig. 4.4 show the following:

- At lower frequencies, the approximation is very good.
- As the frequency increases, approaching and exceeding the "pumping" frequency (2 Hz), the periodic control signal starts to interact significantly with the harmonics of the LTP system, destroying the equivalence of the nonlinear system and its LTI simplification.

Chapter 5

Summary

We developed a framework to recover observability via active sensing using HTF theory. Our central idea is that the higher harmonics of an active sensing system render the system observable. To illustrate this, we developed a biologically inspired active sensing system, where the output is a high-pass-filtered point measurement of the sensory scene. Controlling this system to a fixed point is shown to render it non-linearly unobservable. The proposed active sensing framework involves modulation, demodulation, and low-pass filtering the original system. This process transforms the system into an equivalent observable system, thereby recovering its observability.

This framework creates higher harmonics with observable states and then demodulates those dynamics to "base band". To illustrate this framework, we first presented the "simplest" biologically inspired system that requires active sensing. This system was chosen as it is easy to model, and thus enabled us to analytically calculate the

HTF's of the system. With this system in hand, we applied the framework to extract the first harmonic and as predicted, the resulting output now rendered the states of the system observable. Using this observable LTI plant, we demonstrated the effectiveness of the framework by using a standard LQG controller to successfully control the system.

With the framework now developed, future work can delve deeper into designing a more appropriate sensor model than the simple differentiator model as used in this work. Also, the choice of demodulating signal we chose to isolate the observable harmonic can be chosen such that it optimizes some meaningful metric of the system such as an observability metric.

Appendix A

Always Unobservable Sensory Scene

Equation (2.3) shows the need for active sensing ($x_2 \neq 0$). But, it also can be used to derive a non-trivial sensory scene which is always nonlinearly unobservable:

$$(g'(x_1))^2 - g(x_1)g''(x_1) = 0$$

$$\int \frac{g''}{g'} = \int \frac{2g'}{g}$$

$$\log g' = 2\log g + c_1$$

$$\log \frac{g'}{2g^2} = c_1$$

$$g' = c_2 g^2$$

$$\frac{dg}{dx} = c_2 g^2$$
$$\frac{dg}{g^2} = c_2 dx$$
$$\frac{-1}{g} = c_2 x + c_3$$
$$g(x) = \frac{-1}{c_2 x + c_3}$$
$$\implies s(x) = -\frac{1}{c_2} \log(c_2 x + c_3).$$

So, for the system and the derivative sensor chosen in this work, in addition to the trivial case of a constant sensory scene, a logarithmically varying sensory scene also seems to render the system always nonlinearly unobservable.

Appendix B

HTF of the System Using Impulse Response Functions

Möllerstedt [59] demonstrated that Impulse response functions of an LTP system can also be used derive its HTF components. We briefly summarize it here and compare the results to those derived for our active sensing system in Chapter 3.

The output of an LTP system using its impulse response functions can be represented as:

$$y(t) = \int_0^t h(t,\tau)u(\tau)d\tau. \tag{B.1}$$

APPENDIX B. HTF VIA IMPULSE RESPONSE FUNCTIONS

For LTP system,

$$\begin{aligned} h(t+T,\tau+T) &= h(t,\tau), \\ \implies h(t+T,t-r+T) &= h(t,t-r). \end{aligned} \tag{B.2}$$

Therefore, $h(t,t-r)$ is periodic in T. Now,

$$\begin{aligned} h(t,t-r) &= \sum h_k(r)e^{jk\omega_o t}, \\ \implies h(t,\tau) &= \sum h_k(t-\tau)e^{jk\omega_o t}. \end{aligned} \tag{B.3}$$

The output can now be expressed as,

$$\begin{aligned} y(t) &= \int_0^t h(t,\tau)u(\tau)d\tau \\ &= \int_0^t \sum h_k(t-\tau)e^{jk\omega_o t}u(\tau)d\tau \\ &= \int_0^t \sum h_k(t-\tau)e^{jk\omega_o(t-\tau)}u(\tau)e^{jk\omega_o\tau}d\tau \\ &= \sum \int_0^t h_k(t-\tau)e^{jk\omega_o(t-\tau)}u(\tau)e^{jk\omega_o\tau}d\tau \\ &= \sum_k \left(h_k(t) * u(t)\right)e^{jk\omega_o t}, \end{aligned} \tag{B.4}$$

where h_k's are the Fourier coefficients of $h(t,t-r)$.

Now, for our active sensing system (2.5), we have

$$\begin{aligned} h(t, t-r) &= C(t)\Phi(t, t-r)B \\ &= C(t) \begin{bmatrix} 1 & (1-e^{-br/m})\frac{m}{b} \\ 0 & e^{-br/m} \end{bmatrix} \begin{bmatrix} 0 \\ \frac{1}{m} \end{bmatrix} \\ &= C(t) \begin{bmatrix} (1-e^{-br/m})\frac{1}{b} \\ \frac{1}{m}e^{-br/m} \end{bmatrix} \\ &= C(t)\alpha(r). \end{aligned} \tag{B.5}$$

Therefore, $h_k(r) = C_k.\alpha(r)$ where C_k are the Fourier coefficients of $C(t)$. For $g(x) = d_1x + e_1$, it is easy to show that the Fourier coefficients of $C(t)$ are as given in (3.7), and $H_k(s)$, the Laplace transform of h_k $(k = 0, -1, 1)$ is given as shown in (3.8), derived via harmonic balance in Chapter 3.

Bibliography

[1] R. Bajcsy, "Active perception," *Proc IEEE*, vol. 76, no. 8, pp. 966–1005, 1988.

[2] M. E. Nelson and M. A. MacIver, "Sensory acquisition in active sensing systems," *J Comp Physiol A*, vol. 192, no. 6, pp. 573–586, 2006.

[3] S. A. Stamper, E. Roth, N. J. Cowan, and E. S. Fortune, "Active sensing via movement shapes spatiotemporal patterns of sensory feedback," *J Exp Biol*, vol. 215, no. 9, pp. 1567–1574, 2012.

[4] R. Ditchburn and B. Ginsborg, "Vision with a stabilized retinal image," *Nature*, vol. 170, no. 4314, pp. 36–37, 1952.

[5] C. F. Moss and A. Surlykke, "Auditory scene analysis by echolocation in bats," *J Acoust Soc Am*, vol. 110, no. 4, pp. 2207–2226, 2001.

[6] N. Ulanovsky and C. F. Moss, "What the bat's voice tells the bat's brain," *Proc Nat Acad Sci*, vol. 105, no. 25, pp. 8491–8498, 2008.

BIBLIOGRAPHY

[7] T. H. Bullock, "Electroreception," *Annu Rev Neurosci*, vol. 5, no. 1, pp. 121–170, 1982.

[8] E. Ahissar and A. Arieli, "Figuring space by time," *Neuron*, vol. 32, no. 2, pp. 185–201, 2001.

[9] L. J. Fleishman and A. C. Pallus, "Motion perception and visual signal design in anolis lizards," *Proc Nat Acad Sci*, vol. 277, no. 1700, pp. 3547–3554, 2010.

[10] K. Ghose and C. F. Moss, "Steering by hearing: a bats acoustic gaze is linked to its flight motor output by a delayed, adaptive linear law," *J Neurosci*, vol. 26, no. 6, pp. 1704–1710, 2006.

[11] P. König and H. Luksch, "Active sensing-closing multiple loops," *Zeitschrift für Naturforschung C*, vol. 53, no. 7-8, pp. 542–549, 1998.

[12] S. J. Lederman and R. L. Klatzky, "Hand movements: A window into haptic object recognition," *Cog Psych*, vol. 19, no. 3, pp. 342–368, 1987.

[13] P. Madsen, I. Kerr, and R. Payne, "Echolocation clicks of two free-ranging, oceanic delphinids with different food preferences: false killer whales *Pseudorca crassidens* and Risso's dolphins *Grampus griseus*," *J Exp Biol*, vol. 207, no. 11, pp. 1811–1823, 2004.

[14] J. Najemnik and W. S. Geisler, "Optimal eye movement strategies in visual search," *Nature*, vol. 434, no. 7031, pp. 387–391, 2005.

[15] R. Peters, W. Loos, F. Bretschneider, and A. Baretta, "Electroreception in catfish: patterns from motion," *Belg J Zool*, no. 1, 1999.

[16] K. Sathian, "Tactile sensing of surface features," *Trends Neurosci*, vol. 12, no. 12, pp. 513–519, 1989.

[17] C. E. Schroeder, D. A. Wilson, T. Radman, H. Scharfman, and P. Lakatos, "Dynamics of active sensing and perceptual selection," *Curr Opin Neurobiol*, vol. 20, no. 2, pp. 172–176, 2010.

[18] C. Assad, B. Rasnow, and P. K. Stoddard, "Electric organ discharges and electric images during electrolocation," *J Exp Biol*, vol. 202, no. 10, pp. 1185–1193, 1999.

[19] D. Babineau, J. E. Lewis, and A. Longtin, "Spatial acuity and prey detection in weakly electric fish," *PLoS Comp Biol*, vol. 3, no. 3, p. e38, 2007.

[20] W. Heiligenberg, "Theoretical and experimental approaches to spatial aspects of electrolocation," *J Comp Physiol*, vol. 103, no. 3, pp. 247–272, 1975.

[21] M. A. MacIver, N. A. Patankar, and A. A. Shirgaonkar, "Energy-information trade-offs between movement and sensing," *PLoS Comp Biol*, vol. 6, no. 5, p. e1000769, 2010.

[22] E. Ahissar and A. Arieli, "Seeing via miniature eye movements: a dynamic hypothesis for vision," *Frontiers Comp Neurosci*, vol. 6, p. 89, 2012.

[23] D. H. Ballard, "Animate vision," *Artif Intell*, vol. 48, no. 1, pp. 57–86, 1991.

[24] A. Blake and A. Yuille, Eds., *Active Vision*. Cambridge, MA, USA: MIT Press, 1993.

[25] M. Brecht, B. Preilowski, and M. M. Merzenich, "Functional architecture of the mystacial vibrissae," *Behav Brain Res*, vol. 84, no. 1, pp. 81–97, 1997.

[26] G. E. Carvell and D. Simons, "Biometric analyses of vibrissal tactile discrimination in the rat," *J Neurosci*, vol. 10, no. 8, pp. 2638–2648, 1990.

[27] R. A. Grant, B. Mitchinson, C. W. Fox, and T. J. Prescott, "Active touch sensing in the rat: anticipatory and regulatory control of whisker movements during surface exploration," *J Neurophysiol*, vol. 101, no. 2, pp. 862–874, 2009.

[28] J. W. Gustafson and S. L. Felbain-Keramidas, "Behavioral and neural approaches to the function of the mystacial vibrissae." *Psychol Bull*, vol. 84, no. 3, p. 477, 1977.

[29] M. J. Hartmann, "Active sensing capabilities of the rat whisker system," *Auton Robot*, vol. 11, no. 3, pp. 249–254, 2001.

[30] V. Dürr, Y. König, and R. Kittmann, "The antennal motor system of the stick insect carausius morosus: anatomy and antennal movement pattern during walking," *J Comp Physiol A*, vol. 187, no. 2, pp. 131–144, 2001.

[31] B. Horseman, M. Gebhardt, and H. Honegger, "Involvement of the suboe-

sophageal and thoracic ganglia in the control of antennal movements in crickets," *J Comp Physiol A*, vol. 181, no. 3, pp. 195–204, 1997.

[32] T. J. Prescott, M. E. Diamond, and A. M. Wing, "Active touch sensing," *Philos Trans R Soc B*, vol. 366, no. 1581, pp. 2989–2995, 2011.

[33] A. Saig, G. Gordon, E. Assa, A. Arieli, and E. Ahissar, "Motor-sensory confluence in tactile perception," *J Neurosci*, vol. 32, no. 40, pp. 14 022–14 032, 2012.

[34] S. Ranade, B. Hangya, and A. Kepecs, "Multiple modes of phase locking between sniffing and whisking during active exploration," *J Neurosci*, vol. 33, no. 19, pp. 8250–8256, 2013.

[35] M. Wachowiak, "All in a sniff: olfaction as a model for active sensing," *Neuron*, vol. 71, no. 6, pp. 962–973, 2011.

[36] D. W. Wesson, T. N. Donahou, M. O. Johnson, and M. Wachowiak, "Sniffing behavior of mice during performance in odor-guided tasks," *Chem Senses*, vol. 33, no. 7, pp. 581–596, 2008.

[37] E. S. Hassan, "Hydrodynamic imaging of the surroundings by the lateral line of the blind cave fish *Anoptichthys jordani*," in *The Mechanosensory Lateral Line*. Springer, 1989, pp. 217–227.

[38] J. C. Montgomery, S. Coombs, and C. F. Baker, "The mechanosensory lateral line

system of the hypogean form of astyanax fasciatus," in *The biology of hypogean fishes*. Springer, 2001, pp. 87–96.

[39] C. Von Campenhausen, I. Riess, and R. Weissert, "Detection of stationary objects by the blind cave fish *Anoptichthys jordani* (*Characidae*)," *J Comp Physiol*, vol. 143, no. 3, pp. 369–374, 1981.

[40] J. Aloimonos, I. Weiss, and A. Bandyopadhyay, "Active vision," *Int J Comp Vis*, vol. 1, no. 4, pp. 333–356, 1988.

[41] P. Gao, B. Ploog, and H. Zeigler, "Whisking as a "voluntary" response: operant control of whisking parameters and effects of whisker denervation," *Somatosens Mot Res*, vol. 20, no. 3-4, pp. 179–189, 2003.

[42] J. J. Gibson, "Observations on active touch." *Psychol Rev*, vol. 69, no. 6, p. 477, 1962.

[43] C. B.-C. Hille, G. Dücker, and P. Guido Dehnhardt, "Haptic discrimination of size and texture in squirrel monkeys (*Saimiri sciureus*)," *Somatosens Mot Res*, vol. 18, no. 1, pp. 50–61, 2001.

[44] M. Lungarella, T. Pegors, D. Bulwinkle, and O. Sporns, "Methods for quantifying the informational structure of sensory and motor data," *Neuroinformatics*, vol. 3, no. 3, pp. 243–262, 2005.

[45] C. E. Raburn, K. J. Merritt, and J. C. Dean, "Preferred movement patterns

during a simple bouncing task," *J Exp Biol*, vol. 214, no. 22, pp. 3768–3774, 2011.

[46] E. Visalberghi and C. Néel, "Tufted capuchins (*Cebus apella*) use weight and sound to choose between full and empty nuts," *Ecol Psychol*, vol. 15, no. 3, pp. 215–228, 2003.

[47] N. J. Cowan and E. S. Fortune, "The critical role of locomotion mechanics in decoding sensory systems," *J Neurosci*, vol. 27, no. 5, pp. 1123–1128, 2007. [Online]. Available: http://dx.doi.org/10.1523/JNEUROSCI.4198-06.2007

[48] S. Sefati, I. D. Neveln, E. Roth, T. R. Mitchell, J. B. Snyder, M. A. MacIver, E. S. Fortune, and N. J. Cowan, "Mutually opposing forces during locomotion can eliminate the tradeoff between maneuverability and stability," *Proc Nat Acad Sci*, vol. 110, no. 47, pp. 18 798–18 803, 2013.

[49] N. J. Cowan, M. M. Ankarali, J. P. Dyhr, M. S. Madhav, E. Roth, S. Sefati, S. Sponberg, S. A. Stamper, E. S. Fortune, and T. L. Daniel, "Feedback control as a framework for understanding tradeoffs in biology," *Integr Comp Biol*, vol. 54, no. 2, pp. 223–237, 2014. [Online]. Available: http://icb.oxfordjournals.org/cgi/doi/10.1093/icb/icu050

[50] E. Roth, K. Zhuang, S. A. Stamper, E. S. Fortune, and N. J. Cowan, "Stimulus predictability mediates a switch in locomotor smooth pursuit performance for *Eigenmannia virescens*." *J Exp Biol*, vol. 214, no. 7, pp. 1170–1180, 2011.

[51] S. C. Whitehead, T. Beatus, L. Canale, and I. Cohen, "Pitch perfect: how fruit flies control their body pitch angle," *J Exp Biol*, vol. 218, no. 21, pp. 3508–3519, 2015.

[52] H. Nijmeijer and A. Van der Schaft, *Nonlinear dynamical control systems*. Springer Science & Business Media, 2013.

[53] B. T. Hinson, M. K. Binder, and K. A. Morgansen, "Path planning to optimize observability in a planar uniform flow field," in *Proc Amer Control Conf*. IEEE, 2013, pp. 1392–1399.

[54] S. Cedervall and X. Hu, "Nonlinear observers for unicycle robots with range sensors," *IEEE Trans Autom Control*, vol. 52, no. 7, p. 1325, 2007.

[55] N. M. Wereley, "Analysis and control of linear periodically time varying systems," Ph.D. dissertation, Massachusetts Institute of Technology, 1990.

[56] M. M. Ankarali and N. J. Cowan, "System identification of rhythmic hybrid dynamical systems via discrete time harmonic transfer functions," in *Proc IEEE Int Conf on Decision Control*. IEEE, 2014, pp. 1017–1022.

[57] A. Siddiqi, "Identification of the harmonic transfer functions of a helicopter rotor," Ph.D. dissertation, Massachusetts Institute of Technology, 2001.

[58] N. M. Wereley and S. R. Hall, "Frequency response of linear time periodic systems," in *Proc IEEE Int Conf on Decision Control*. IEEE, 1990, pp. 3650–3655.

[59] E. Möllerstedt, "Dynamic analysis of harmonics in electrical systems," Ph.D. dissertation, Lund University, 2000.

[60] S. Butterworth, "On the theory of filter amplifiers," *Wireless Engineer*, vol. 7, no. 6, pp. 536–541, 1930.

[61] R. E. Kalman, "A new approach to linear filtering and prediction problems," *Trans ASME*, vol. 82, no. Series D, pp. 35–45, 1960.

Vita

Abhinav Kunapareddy received his B. Tech. degree in Mechanical Engineering from Indian Institute of Technology Madras, India in 2014, and enrolled in the Mechanical engineering M.S.E. program at Johns Hopkins University the same year. He is currently associated with the Locomotion in Mechanical and Biological Systems (LIMBS) Laboratory, Johns Hopkins University. His current research interests include optimal control, estimation and bio-inspired robotics.